


Research Article

The Potential Mechanism of Zishen Yutai Pills against Threatened Abortion: An Approach Involving Network Pharmacology and Experimental Evidence

Jiazhen Wang,^{1,2} Xin Liu,^{1,2} Yougang Zhang,³ Shenghua Lin,^{1,2} Honglin Ma,^{1,2} Ting Lei,⁴ Chen Sun,¹ Kechun Liu,¹ and Qiuxia He^{1,2} 

¹Science and Technology Service Platform, Qilu University of Technology (Shandong Academy of Sciences), Jinan, Shandong, China

²Biology Institute, Science and Technology Service Platform of Shandong Academy of Sciences, Qilu University of Technology (Shandong Academy of Sciences), Jinan, Shandong, China

³School of Pharmacy and Pharmaceutical Sciences, Shandong First Medical University, Jinan, Shandong, China

⁴Guangzhou Baiyunshan Zhongyi Pharmaceutical Co., Ltd., Guangzhou, China

Correspondence should be addressed to Qiuxia He; heqiuxia2022@126.com

Jiazhen Wang and Xin Liu contributed equally to this work.

Received 16 August 2022; Revised 3 December 2022; Accepted 13 December 2022; Published 31 January 2023

Academic Editor: Rajeev K. Singla

Copyright © 2023 Jiazhen Wang et al. This is an open access article distributed under the Creative Commons Attribution License, which permits unrestricted use, distribution, and reproduction in any medium, provided the original work is properly cited.

Threatened abortion (TA) is the most common complication in early pregnancy and is caused by anxiety and depressive symptoms. The Zishen Yutai Pill (ZYP) is a traditional herbal formula that is commonly used to treat TA. However, the pharmacological mechanisms underlying the effect of ZYP have yet to be elucidated. To disclose the mechanism of ZYP in the treatment of TA, first, we identified the chemical constituents of ZYP from multiple databases and then predicted the potential targets of TA by applying the GeneCards database. A protein-protein interaction (PPI) network was then constructed to allow the screening of hub targets. Gene Ontology (GO) and Kyoto Encyclopedia of Genes and Genomes (KEGGs) enrichment analyses were also performed and the Database for Annotation Visualization and Integrated Discovery server was used to identify critical biological processes and signaling pathways. Cytoscape software was used to construct a Compound-Target-Pathway. Furthermore, we analyzed ZYP by UPLC-Q-TOF/MS, then the RU486-induced TA rat model was established, and the reliability of the network pharmacology prediction results was verified. Finally, the mechanisms responsible for the action of ZYP on TA were revealed by qRT-PCR and molecular docking. Database screening identified a total of 161 active compounds in ZYP and 324 TA-related targets. And, we identified 42 compounds from ZYP by UPLC-Q-TOF/MS. Inflammation and apoptosis were identified as the main biological processes. GO and KEGG analyses identified that the MAPK and PI3K/Akt pathways were the key functional pathways that respond to ZYP. The results showed that ZYP treatment significantly increased maternal weight, significantly increased the levels of estradiol and progesterone, and attenuated histopathological changes in a rat model of TA. Data indicated that ZYP treatment improved pregnancy outcomes in the rat model of TA. QRT-PCR data showed that ZYP reduced inflammation and apoptosis by regulating the MAPK and PI3K/Akt pathways. In addition, molecule docking results identified a range of key compounds, including *Pik3a*, *Mapk14*, *Mapk1*, *Mapk3*, *Mapk8*, *Tnf*, *Il6*, and *Cas8*. In summary, we performed network pharmacological analysis and experimental validation and identified that ZYP exerts an effect on TA by regulating the MAPK and PI3K/Akt pathways and by inhibiting the expression levels of proinflammatory cytokines and genes related to apoptosis.

1. Introduction

Threatened abortion (TA) is defined as the occurrence of vaginal bleeding before 20 weeks of gestation, with or without lower abdominal pain or back pain. TA is a common complication in early pregnancy with a morbidity rate of approximately 20% [1, 2]. A closed cervix and a viable intrauterine fetus are the prerequisites for TA [3]. Many risk factors are thought to contribute to TA, including uterine malformation [4], chromosome aberration [5, 6], dysfunctions of the immune system [7, 8], certain maternal infections [9], and endocrine disturbance [10]. Threatened abortion may cause both physical and psychological impacts on the mother, including the development of depressive symptoms, anxiety, and obsessive-compulsive disorder [11].

As a well-known traditional Chinese medicine, Zishen Yutai Pills (ZYP) were first invented by Professor Yuankai Luo in 1983 and consist of *Cuscutae Semen*, *Amomi Fructus*, *Rehmanniae Radix Praeparata*, *Ginseng Radix et Rhizoma*, *Taxilli Herba*, *Asini Corii Colla*, *Polygoni multiflori Radix Praeparata*, *Artemisiae argyi Folium*, *Morindae officinalis Radix*, *Atractylodis macrocephalae Rhizoma*, *Codonopsis Radix*, *Cervi Cornu Degelatinatum*, *Lycii Fructus*, *Dipsaci Radix*, and *Eucommiae Cortex* (detailed herbal information of ZYP is listed in Table 1). The convincing evidence from Clinical practice shows that the use of ZYP on patients undergoing in vitro Fertilization-embryo transfer can enhance endometrial receptivity and improve embryonic implantation [12, 13] and treat TA and infertility [14, 15]. ZYP can also promote the supply of blood to gonads and the development of follicles and the corpus luteum and improve luteal phase defects, menstrual disorders, and ovarian dysfunction [16, 17]. ZYP has been demonstrated to reduce the follicle-stimulating hormone and significantly increase the estradiol and progesterone in serum levels of infertile women with polycystic ovary syndrome, thus improving the fertility rate of patients [18, 19]. Although ZYP is gaining an increasingly prominent reputation for its clinical application, the mechanisms responsible for its action have yet to be elucidated.

Over recent years, network pharmacology has become widely used in Traditional Chinese Medicine (TCM) research, with a strong emphasis on holistic treatment, a systematic approach, and drug interactions [20]; these concepts underlie the very nature of TCM. Network pharmacology applied web-based approaches and relied on computational simulation for data mining and molecular docking to systematically elucidate the effects and intervention of drugs on disease networks [21, 22]. Network pharmacology provides a new concept for studying multi-targeted mechanisms when using TCM to treat complex diseases, including TA.

The onset of TA will directly lead to the occurrence of miscarriage once it is not treated promptly and effectively. Although there are various reports describing the therapeutic effects of ZYP in clinical practice, studies on the mechanism of action of ZYP are lacking. Hence, we still need to determine the specific molecular mechanism of ZYP action on TA. In this study, we used network pharmacology methods to investigate the mechanisms underlying the effect

of ZYP on TA. We then validated our predictions in an animal model of TA to identify potential mechanisms.

2. Materials and Methods

2.1. Molecular Database Building of ZYP. The total of chemical ingredients of ZYP (15 Herbs) was retrieved from the Traditional Chinese Medicines for Systems Pharmacology Database (TCMSP, <https://tcmsp.com>) and Shanghai Institute of Organic Chemistry of the Chinese Academy of Sciences Chemistry Database (<https://www.organchem.csdb.cn>).

2.2. The Screening of Active Ingredients

2.2.1. Oral Bioavailability. Oral bioavailability (OB) was defined as the proportion (%) of unmodified drugs that enter the systemic circulation after oral administration. OB has become an important pharmacokinetic parameter identifying candidate compounds that can be developed into drugs [23]. Ingredients with an $OB \geq 30\%$ were selected as potential ingredients for subsequent research.

2.2.2. Evaluation of Drug-Likeness. Drug-likeness (DL) refers to the similarity between ingredients and known drugs [24, 25]. The DL values of the molecules in ZYP were evaluated by the Tanimoto coefficient by applying the following equation [26]:

$$f(a, b) = \frac{a \times b}{a^2 + b^2 - a \times b}. \quad (1)$$

Here, a refers to the herbal ingredients and b represents the average molecular properties for all ingredients according to the DrugBank database [27, 28]; ingredients with a $DL \geq 0.18$ were selected for the next study. When compounds met both criteria ($OB \geq 30\%$ and $DL \geq 0.18$), they were regarded as candidate compounds for subsequent analysis [23, 29].

2.3. The Prediction of ZYP Chemical Compound Targets. To identify precise target genes of ZYP, all active ingredients of ZYP that had been screened by OB and DL were individually retrieved in the PubChem database (<https://pubchem.ncbi.nlm.nih.gov/>) to obtain a range of information, including molecular formula, molecular weight, and canonical simplified molecular-input line-entry specification (SMILES). We also entered SMILES data for each compound into Swiss Target Prediction (<http://www.swisstargetprediction.ch/>). We found that it was necessary to check whether the compound structures identified in PubChem and Swiss Target Prediction databases were consistent. To ensure consistency, all targets of compounds with probability > 0 were retained from the Swiss Target Prediction database for subsequent analysis.

2.4. The Prediction of TA Targets. Targets related to TA were retrieved from the OMIM databases (<https://omim.org/>) and GeneCards databases (<https://www.genecards.org/>). Then, the common matched targets of ZYP targets and TA disease genes were acquired and drew a Venn diagram showing the

TABLE 1: The sequences of primer pairs were used in the real-time quantitative PCR assay.

No.	Gene symbol	Forward primer	Reverse primer
1	<i>β-actin</i>	ACTGCCGCATCCTCTTCCTC	CTCCTGCTTGCTGATCCACATC
2	<i>Casp3</i>	CGGACCTGTGGACCTGAAAA	CGGCCTCCACTGGTATCTTC
3	<i>Casp8</i>	AACGTCTGGGCAACGAAGAA	ATCCCGCCGACTGATATGGA
4	<i>Il6</i>	TTTCTCTCCGCAAGAGACTTCC	TGTGGGTGGTATCCTCTGTGA
5	<i>Jun</i>	GCACATCACCACTACACCGA	TATGCAGTTCAGCTAGGGCG
6	<i>Erk2</i>	AATGTTCTGCACCGTGACCT	TGGTCTGGATCTGCAACACG
7	<i>Mapk14</i>	GCAACCTCGCTGTGAATGAA	CACGTAGCCGGTCATTTTCGT
8	<i>Erk1</i>	CACTGGCTTTCTGACCGAGT	GCCACAGACCAGATGTCAA
9	<i>Mapk8</i>	ACAGACCTAAGTACGCTGGC	ACCAGACGTTGATGTACGGG
10	<i>Pik3ca</i>	ACCTCAGGCTTGAAGAGTGTC	CAGATGTTCTCCATGATTCCGA
11	<i>Tnf</i>	ATGGGCTCCCTCTCATCAGT	GCTTGGTGGTTTGTCTACGAC
12	<i>Akt1</i>	AGCTGATGAAGACAGAGCGG	GACCGGAAGTCCATCGTCTC

intersecting genes (<https://bioinformatics.psb.ugent.be/webtools/Venn/>) [30].

2.5. Network Topological Feature Analyses. We chose overlapping targets to construct the PPI network. The common targets were processed by STRING (<https://string-db.org/>) to identify interactions between the proteins expressed by target genes, with the organism parameter set as “*Homo sapiens*.” Next, the PPI network of graphical interactions was constructed and visualized using Cytoscape (version 3.6.0, Institute for Systems Biology, Seattle, WA, USA).

2.6. GO Enrichment and KEGG Analysis. The candidate targets for ZYP were imported into the DAVID database (version 6.7, <https://david.ncifcrf.gov/>) for GO functional enrichment analysis and KEGG signaling pathway enrichment analysis, respectively [31, 32]. The analysis identified a range of GO terms, including biological process (BP), molecular function (MF), and cellular components (CC). In this study, the organism parameter was selected as “*Homo sapiens*.” The analysis threshold was set to $p < 0.05$ and FDR < 0.05 .

2.7. Construction of a Compound-Target-Pathway Network. To better investigate the holistic mechanisms underlying the actions of ZYP in the treatment of TA, we used Cytoscape to create a compound-target-pathway network; this allowed us to identify potential interactions. The targets contained in the first 22 pathways, and the compounds corresponding to these targets, were then identified by Cytoscape software [33].

2.8. Reagents. ZYP was provided by the Guangzhou Baiyunshan Zhongyi Pharmaceutical Co., Ltd. (Batch 20191024, Guangzhou, China). The ZYP sample has been deposited in the Key Laboratory for Drug Screening Technology of Shandong Academy of Sciences, Jinan, Shandong, China. Dydrogesterone Tablets were purchased from Abbott Healthcare Product B.V. (Batch No.361768, The Netherlands). Mifepristone was purchased from Shanghai Yuanye Bio-Technology Co., Ltd. (purity 98%, Lot: Y02M7D10327, Shanghai, China). Stroke-physiological saline solution was purchased from Shandong Lukang Chenxin Pharmaceutical

CO., Ltd. (Batch H20113370, Shandong, China). Rat Progesterone (P) ELISA Kit and Rat Estradiol (E2) ELISA Kit were purchased from Jiangsu Mei Biao Biological Technology Co., Ltd. (Batch MB-6832A and MB-2116A, Jiangsu, China).

2.9. Analysis of ZYP by UPLC-Q-TOF-MS. The main chemical components of the ZYP aqueous extract sample were analyzed by the UPLC-Q-TOF-MS system equipped. Weighed ZYP 0.5 g, added 80% methanol 10 ml, sonicated (power 300 W, frequency 40 kHz) for 30 min, let cool, shaken well, centrifuged (12000 rpm) for 5 min, and the supernatant was the test solution. The mobile phase was acetonitrile (A) and 0.1% aqueous formic acid (B), with a gradient elution procedure as follows. The flow rate was 0.3 mL/min, and the column temperature was 30°C, the injection volume was 1 μ L. 100% B at 0–3 min; 100%–94% B at 3–5 min; 94% B at 5–7 min; 94%–85% B at 7–15 min; 85%–80% B at 15–30 min; 80%–65% B at 30–40 min; 65%–55% B at 40–45 min; 55%–25% B at 45–50 min; 25%–10% B at 50–55 min; 10% B at 55–57 min; 10%–100% B at 57–57.1 min; and 100% B at 57.1–60 min. The MS analysis was carried out with the electrospray ionization (ESI) source in both positive and negative ion modes. The instrumental settings of Q-TOF-LC-MS were as follows: the gas temperature was 325°C. Collision energy spread (CES) was 40 eV. Drying Gas and Sheath Gas were set to 8 L/min, Nozzle Voltage was set to 1000 V, Fragmentor was set to 175 V, and Skimmer was set to 60 V. Data were analyzed by MassHunter Workstation Software Qualitative Analysis (version 10.0) software.

2.10. In Vivo Animal Experiment. Sexually mature female and male Sprague–Dawley (SD) rats, aged 9 weeks and weighted 200–260 g, were obtained from the Center of Experimental Animals of Shandong province (certification: SCXK 20190003, Shandong, China). The SD rats were bred under a 12 h light/12 h dark cycle with constant humidity and temperature (25°C) and were adapted for 1 week before experiments with *ad libitum* access to standard food and water. All experiments were approved by the Institutional Animal Ethical Committee of the Biology Institute of Shandong Academy of Sciences (approval number: SWS20201210).

Females in estrus were identified and placed in a cage with males (2:1 ratio) overnight. The next morning, we

checked the females for signs of a vaginal plug. Pregnant rats were randomly allocated into four groups: control, model (RU486), positive control (dydrogesterone, DT), and ZYP. Rats were given 2 mL of stroke-physiological saline solution by gavage every day from day 1 to day 10 in the control group and the RU486 group. Rats in the DT group were given 3.15 mg/kg of DT by gavage every day from days 1 to 10 after pregnancy confirmation as a positive control. Rats in the ZYP group were given 1.575 g/kg of ZYP by gavage daily from days 1 to 10 after fertilization. On the 10th day of pregnancy (except for the control group), the rats in the remaining groups were given 3.75 mg/kg of mifepristone (RU486) to establish the model of abortion. The body weights of rats were recorded on days 1, 5, and 10 after fertilization. SD rats were anesthetized and euthanized after being incubated with RU486 for 24 hours. Following experimentation and sacrifice, the harvested uterine tissue of pregnant rats was weighed and fixed in 4% formaldehyde or immediately frozen in liquid nitrogen and stored at -80°C for the following experiments.

2.11. Biochemistry Analysis of Serum Samples. The blood samples were taken from the abdominal aorta of each rat, centrifuged at 300 rpm for 10 minutes to separate the serum, and then stored at -20°C . Serum samples were subsequently used with ELISA kits to detect E2 and P according to the manufacturer's instructions (Jiangsu Mei Biao Biological Technology Co., Ltd., Jiangsu, China).

2.12. Histopathology. Histopathological evaluation was performed as previously described [34]. Samples of rat uteri were fixed in 4% paraformaldehyde for 48 hours, processed and embedded in paraffin (Beyotime Biotechnology), sliced into slices (4 μm), and stained with hematoxylin and eosin. A light microscope was then used to investigate the endometrial tissue for morphological changes.

2.13. Total RNA Extraction and RT-PCR. Fast Pure Cell/Tissue Total RNA Isolation Kit V2 (Vazyme, Nanjing, China) was used to extract RNA following the instructions. RNA was then reverse transcribed to cDNA using ABScript II Reverse Transcription premixed solution (Abclonal, Wuhan, China). QRT-PCR was then performed using SYBR Green Fast qPCR Mix (Abclonal, Wuhan, China) on a Light Cycler 96 System (Roche, Basel Switzerland). The target mRNA levels were normalized to the β -actin internal control gene. Primer sequences are given in Table 1.

2.14. Molecular Docking. Next, we performed molecular docking to further verify the interaction between key compounds and hub target proteins. The crystallographic structure of a selected target protein was obtained from the RCSB Protein Data Bank (<https://www.pdb.org/>). We then used Puchem to download the two-dimensional structure of the compound. Next, we used Chemdraw to transform the structure into a three-dimensional structure and performed energy minimization. Both the target protein and compound

were processed with Autodock Tools 1.5.6. Finally, Autodock vina was used for batch molecular docking research.

2.15. Statistics Analysis. All experimental data are presented as mean \pm standard error of the mean (SEM). Statistical analysis was performed using SPSS 25.0 statistical software (SPSS Inc., Chicago, IL) and GraphPad Prism 6.0 (GraphPad Software; CA, USA). Statistical tests between multiple datasets were carried out using one-way analysis of variance (ANOVA) followed by Dunnett's posthoc test; $p < 0.05$ or $p < 0.01$ indicated a statistically significant difference.

3. Result

3.1. The Active Compounds in ZYP. We identified a total of 1363 compounds in the fifteen herbs (Table 2) that form ZYP; these were identified by searching the TCMSP and Chemistry databases. After screening all compounds against strict criteria, we identified 161 bioactive compounds with excellent ADME properties.

3.2. Target Prediction and Analysis. During the target prediction process, and after deleting duplications, 142 of the 161 candidate ingredients yielded 1025 targets (19 of the 161 bioactive compounds had no direct targets). The GeneCards database was used to identify the target genes related to human disease; the search term was "threatened abortion." A total of 1732 targets related to TA were identified by the GeneCards database. Figure 1(a) shows a Venn diagram of target genes and indicates that ZYP and TA share 324 target genes.

3.3. Exploration of the Target Genes in the PPI. The PPI data calculated by STRING were input into Cytoscape software to establish a potential target-TA-related molecular network for the Chinese medicine contained in ZYP. In total, 324 common targets were identified and used to create a PPI network; there were 320 nodes and 6468 edges in total (Figure 1(b)). During the first round of screening, the thresholds were set to a "Degree Centrality" (DC) ≥ 32 , "Betweenness Centrality" (BC) ≥ 0.000 , and "Closeness Centrality" (CC) ≥ 0.478 . In total, we identified 161 hub nodes and 4146 edges (Figure 1(c)). For the second round of screening, we set the following thresholds: DC ≥ 73.5 , BC ≥ 0.002 , and CC ≥ 0.555 . In total, we obtained 41 hub nodes and 743 edges (Figure 1(d)). In this network, the hub target genes (DC ≥ 73.5) were regarded as key target genes, including *BCL2L1*, *IL2*, *IL6*, *ERBB2*, *EP300*, *TNF*, *ESR1*, *VEGFA*, *MAPK14*, *MAPK1*, *STAT3*, *mTOR*, *PPARG*, *AR*, *ICAM1*, *STAT1*, *CASP3*, *CASP8*, *EGFR*, *MAPK8*, *PTPRC*, *TLR4*, *PIK3CA*, *SRC*, *NOS3*, *KDR*, *MMP9*, *JAK2*, *ALB*, *MDM2*, *TNF*, *JUN*, *TP53*, *AKT1*, *FGF2*, *HSP90AA1*, *MMP2*, *CCND1*, *SIRT1*, *GAPDH*, and *PTGS2*.

3.4. GO and KEGG Pathway Enrichment Analysis. To ascertain if the 41 gene symbols were related to TA, we conducted GO enrichment analyses using the DAVID database the pathway to identify 169 BPs, 17 CCs, and 32 MFs of significance ($p < 0.05$, and $FDR < 0.05$, Supplementary

TABLE 2: The detailed information about ZYP.

No.	Chinese name	Latin name	English name	Weight ratio (%)
1	Renshen	<i>Panax ginseng</i> C. A. Mey	Ginseng radix et rhizome	1.0
2	Tusizi	<i>Cuscuta chinensis</i> Lam.	Cuscutae semen	15.8
3	Sharen	<i>Amomum villosum</i> Lour.	Amomi fructus	1.6
4	Shudihuang	<i>Rehmannia glutinosa</i> (Gaertn.) DC.	Rehmanniae radix praeparata	10.5
5	Sangjisheng	<i>Taxillus chinensis</i> (DC.) Danser	Taxilli herba	10.5
6	Ejiao	<i>Asini Corii Colla</i>	Asini corii colla	0.7
7	Show	<i>Polygonum multiflorum</i> Thunb.	Polygoni multiflora radix praeparata	10.5
8	Aiye	<i>Artemisia argyi</i> H. Lévl. and vaniot	Artemisiae argyi folium	3.2
9	Bajitian	<i>Morinda officinalis</i> how	Morinda officinalis radix	4.2
10	Baizhu	<i>Atractylodes macrocephala</i> Koidz	Atractylodis macrocephalae rhizoma	5.2
11	Dangshen	<i>Codonopsis pilosula</i> (franch.) Nannf	Codonopsis radix	12.6
12	Lujiaoshuang	<i>Cervus nippon</i> Temminck	Cervi cornu degelatinatum	3.2
13	Gouqizi	<i>Lycium barbarum</i> L.	Lycii fructus	4.2
14	Xuduan	<i>Dipsacus asper</i> Wall. ex DC	Dipsaci radix	10.5
15	Du Zhong	<i>Eucommia ulmoides</i> Oliv	Eucommia cortex	6.3

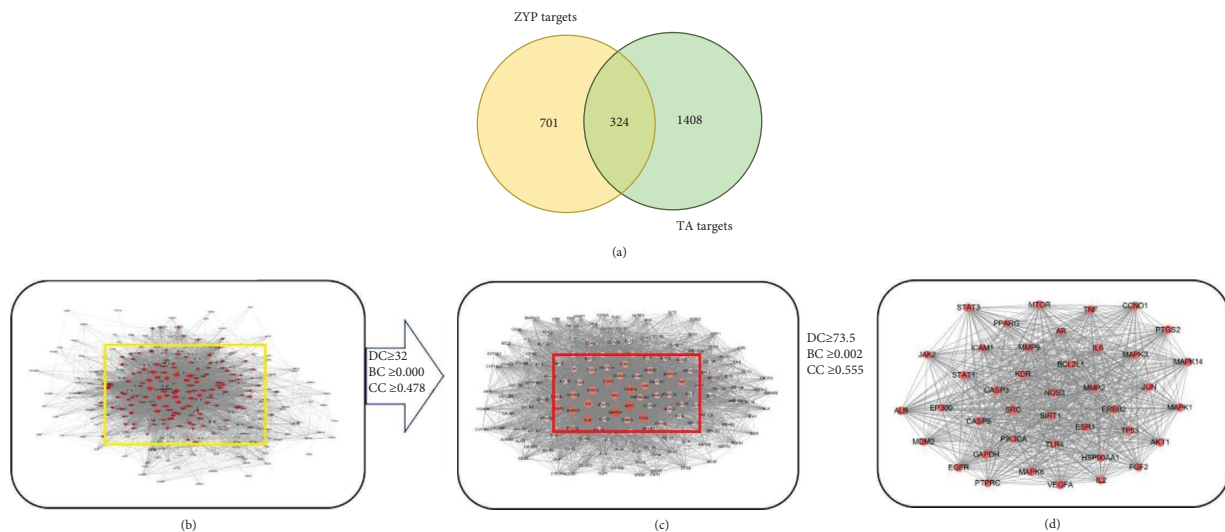


FIGURE 1: The construction of PPI networks. (a) Venn diagram of drug and disease relationship: yellow represents 1025 ZYP-related targets and green represents 1732 targets of TA. The intersection of two circles represents 324 common targets. (b–d) The process of topological screening for the PPI network.

Tables S1–S3). For example, taking the first ten terms with $p < 0.05$ and $FDR < 0.05$ (Figure 2(a)), GO enrichment analyses showed that for BP, these ten terms were mainly involved in the positive regulation of nitric-oxide biosynthetic process (GO: 0045429), protein phosphorylation (GO: 0001934), the ERK1 and ERK2 cascade (GO: 0070374), gene expression (GO: 0010628), smooth muscle cell proliferation (GO: 0048661), transcription from RNA polymerase II promoter (GO: 0045944), response to drugs (GO: 0042493), cellular response to hypoxia (GO: 0071456), the lipopolysaccharide-mediated signaling pathway (GO: 0031663), and the negative regulation of the apoptotic process (GO: 0043066). The MFs of these first ten terms mainly involved protein phosphatase binding (GO: 0019903), protein tyrosine kinase activity (GO: 0004713), nitric-oxide synthase regulator activity (GO: 0030235), kinase activity (GO: 0016301), scaffold protein binding (GO:

0097110), transcription factor binding (GO: 0008134), enzyme binding (GO: 0019899), identical protein binding (GO: 0042802), MAP binding (GO: 0004707), and protein binding (GO: 0005515). With regards to CC, the first ten terms were mainly concentrated in the nucleus, cytosol, nucleoplasm, membrane rafts, caveola, cytoplasm, protein complexes, nuclear chromatin, perinuclear region of the cytoplasm, and mitochondria.

To further identify the potential mechanisms underlying the effect of ZYP on TA, we conducted the KEGG pathway enrichment analysis on 41 targets and identified 104 pathways in the DAVID database ($p < 0.05$, and $FDR < 0.05$, Supplementary Table S4). For example, we took the first 22 terms according to p -value to create bubble charts (Figure 2(b)). Results indicated that ZYP exertion its effect TA by hormone metabolism, inflammation, and apoptosis, including the estrogen signaling pathway, ErbB signaling

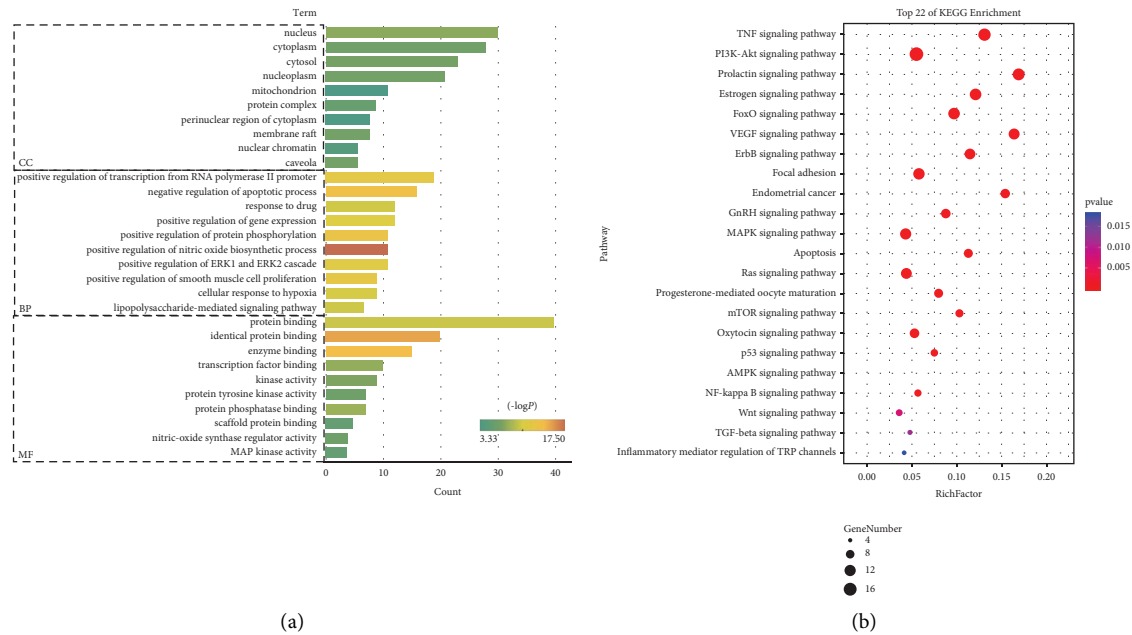


FIGURE 2: Enrichment analysis of potential targets from the main active ingredients of ZYP. (a) GO enrichment of related genes. The X-axis represents the GO terms: CC: cellular component, BP: biological process, and MF: molecular function. Y-axis represents the sizes of the dots representing the gene count of each term; the color scales indicated the different thresholds of adjusted p values. (b) Top 22 pathways enriched by the KEGG method. The X-axis shows the gene number in the given gene set that was annotated to certain pathways, and the y-axis represents the rich factor. The size of the node represents the number of target genes in the pathway and the color of the dot reflects the p value.

pathway, oxytocin signaling pathway, endometrial cancer, PI3K-Akt signaling pathway, NF-kappa B signaling pathway, FoxO signaling pathway, TNF signaling pathway, p53 signaling pathway, and apoptosis.

3.5. Component Target Pathway Network Analysis. A compound-target-pathway network for ZYP is shown in Figure 3. This network had 182 nodes and 661 edges, including 13 compounds, 116 active components, 45 targets, and 22 pathways. The nodes represent active components, targets, and pathways. The edges represent their relationships.

3.6. Identification of the Chemical Constituents in ZYP by UPLC-Q-TOF/MS. Total ion chromatograms (TICs) of ZYP are presented in Figure 4. ZYP samples were analyzed by UPLC-Q-TOF/MS, and 42 compounds were identified from ZYP based on the sample multilevel mass spectrometry information, combined with natural product high-resolution mass spectrometry database and related literature (Table 3).

3.7. ZYP Improved the General Condition of a Rat Model of TA and Decelerated the Development of TA. We established an RU486-induced rat TA model to verify the protective effect and mechanisms associated with ZYP. As shown in Figure 5(a), following the administration of RU486, there was a slight reduction in the weight of rats in the RU486 group on days 5 and 10 when compared with controls. Furthermore, as shown in Figure 5(b), blood stasis was

evident, along with a reduced number of embryos, in pregnant rats in the RU486 group (indicated by the arrows) when compared with the control group. Pathological staining indicated that RU486 induced severe interstitial edema (Figure 5(c)). Conversely, ZYP markedly promoted embryonic development and increased maternal weight. ZYP also attenuated histopathological changes and showed a protective effect against RU486. These results suggested that ZYP treatment, consistent with the effect of DT, inhibits the pregnancy loss induced by RU486 fractions.

3.8. Effect of ZYP on Serum E2 and P Levels. ELISA assays were used to determine the levels of E2 and P in RU486-treated and ZYP-treated rats. As shown in Figures 5(d) and 5(e), the levels of E2 and P in the blood of rats in the model group were significantly reduced compared with the control group, ($p < 0.05$ or $p < 0.01$). The levels of E2 and P in the blood of rats in the DT and ZYP groups were significantly increased compared with the model group ($p < 0.05$ or $p < 0.01$).

3.9. Results of Biological Verification. Based on the results of network pharmacology analysis, animal experiments were designed to verify the partial mechanism of ZYP treatment of TA. We analyzed the expression levels of key genes in our experimental rats by qRT-PCR, including *Pi3kca*, *Akt*, *Tnf*, *Il6*, *Cas3*, *Cas8*, *Erk1*, *Erk2*, *Jun*, *Jak*, and *Mapk14*. As shown in Figure 6, the mRNA expression levels of *Pi3kca*, *Akt*, *Erk1*, *Erk2*, *Jun*, *Jak*, *Mapk14*, *Tnf- α* , *Il6*, *Cas3*, and *Cas8* were significantly increased in rats following treatment with

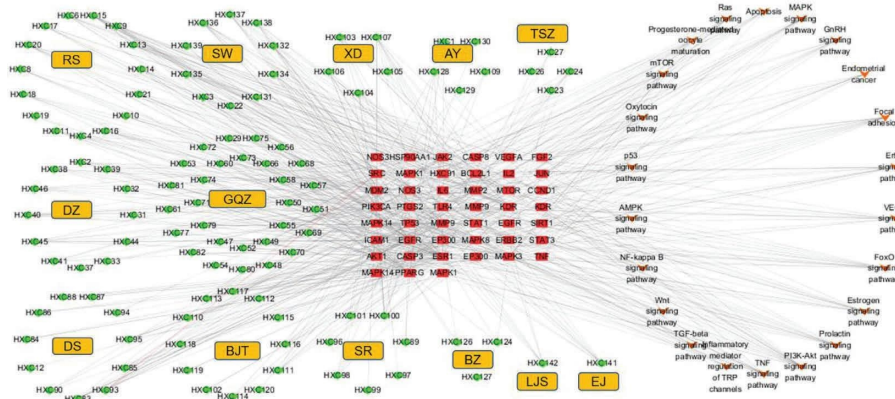


FIGURE 3: Compound-target-pathway network. Green nodes stand for active compounds in ZYP; red nodes stand for known target genes; orange stand for pathway; lines stand for the relationship.

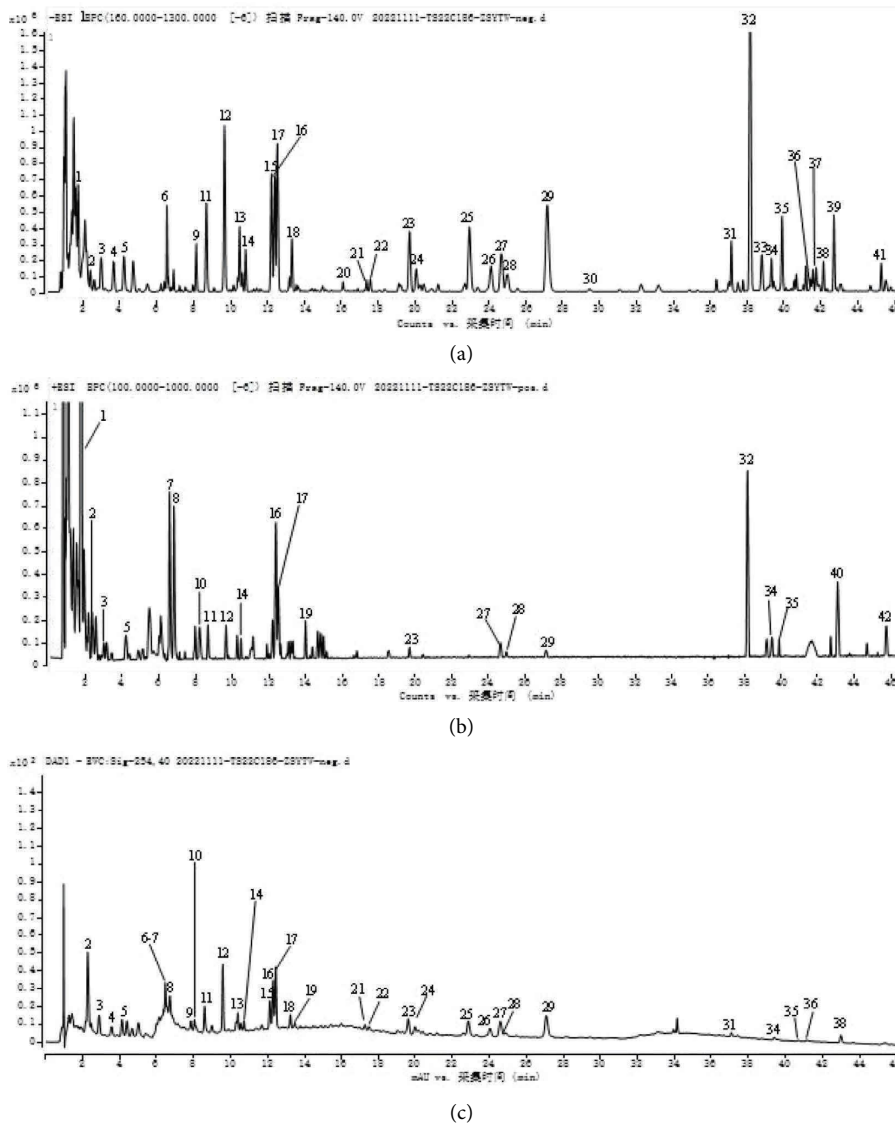


FIGURE 4: The total ion chromatograms total ion chromatogram (TICs) of ZYP by ultraperformance liquid chromatography-quadrupole-time-of-flight tandem mass (UPLC-Q-TOF/MS). (a) TIC of ZYP in negative ion mode; (b) TIC of ZYP in positive ion mode; (c) UPLC chromatogram of ZYP in 254 nm.

TABLE 3: Chemical constituents identified in ZYP based on UPLC-Q-TOF/MS.

No.	Retention time (min)	Ion species	Measured value (m/z)	Theoretical value (m/z)	Δ ppm	Molecular formula	Compound name	MS/MS	Source
1	1.73	$[M + H]^+$	130.0499	130.0499	0.3	$C_5H_7NO_3$	L-pyroglutamic acid	130.0499, 84.0415, 56.0468	A
2	2.38	$[M - H]^-$	243.0618	243.0623	-2.0	$C_9H_{12}N_2O_6$	Uridine	152.0358, 122.0232, 110.0239, 82.0289, 66.0334	D, I, J
3	2.95	$[M - H]^-$	389.1085	389.1089	-1.2	$C_{16}H_{22}O_{11}$	Monotropein	389.1058, 227.0553, 191.0338, 147.0440, 89.0235, 59.0130	G
4	3.63	$[M - H]^-$	389.1086	389.1089	-1.1	$C_{16}H_{22}O_{11}$	Scandoside	389.1070, 227.0553, 209.0445, 165.0551, 137.0598, 59.0130	G
5	4.19	$[M - H]^-$	169.0144	169.0142	0.7	$C_7H_6O_5$	Gallic acid	169.0114, 125.0235, 79.0181, 59.0231	E, F, M
6	6.52	$[M - H]^-$	389.1091	389.1089	0.2	$C_{16}H_{22}O_{11}$	Deacetylasperulosidic acid	389.1080, 227.0552, 209.0441, 183.0658, 165.0549, 89.0235	G, M
7	6.57	$[M + H]^+$	268.1556	268.1543	4.2	$C_{14}H_{21}NO_4$	Codonopsine	161.0500, 121.0556, 88.0678, 58.0577	J
8	6.81	$[M + H]^+$	127.0396	127.0390	4.7	$C_6H_6O_3$	Maltol	127.0388, 109.0228, 81.0336, 53.0383	A
9	8.12	$[M - H]^-$	515.1407	515.1406	0.1	$C_{22}H_{28}O_{14}$	3-O-(3'-O-caffeoyl glucosyl) quinic acid or isomer	515.1393, 341.0864, 179.0343, 135.0440	K, B, M
10	8.22	$[M + H]^+$	247.1445	247.1441	1.6	$C_{14}H_{18}N_2O_2$	Hypaphorine	188.0704, 170.0598, 146.0602, 118.0654, 91.0535, 60.0808	F
11	8.66	$[M - H]^-$	353.0881	353.0878	0.4	$C_{16}H_{18}O_9$	Neochlorogenic acid	353.0864, 191.0556, 179.0342, 135.0445, 85.0286	K, B, M, L, I, H, J
12	9.66	$[M - H]^-$	375.1299	375.1297	0.3	$C_{16}H_{24}O_{10}$	8-Epiloganic acid	375.1289, 213.0764, 169.0860, 113.0237, 69.0340	D
13	10.47	$[M - H]^-$	515.1408	515.1406	-0.1	$C_{22}H_{28}O_{14}$	5-O-(3'-O-caffeoyl glucosyl)quinic acid or isomer	515.1392, 353.0869, 191.0558, 179.0338, 93.0337	K, B, M
14	10.80	$[M - H]^-$	515.1403	515.1406	-0.7	$C_{22}H_{28}O_{14}$	4-O-(3'-O-caffeoyl glucosyl)quinic acid or isomer	515.1389, 353.0866, 341.0866, 191.0558, 179.0343, 173.0448	K, B, M
15	12.20	$[M - H]^-$	353.0884	353.0878	1.5	$C_{16}H_{18}O_9$	Chlorogenic acid	191.0557, 179.0344, 173.0450, 135.0446	K, B, M, L, I, H, J, E
16	12.37	$[M + HCOO]^-$	403.1249	403.1246	0.3	$C_{16}H_{22}O_9$	Sweroside	403.1249, 357.1125, 195.0654, 125.0237, 59.0129	L
17	12.52	$[M - H]^-$	353.0883	353.0878	1.1	$C_{16}H_{18}O_9$	Cryptochlorogenic acid	191.0562, 161.0236, 85.0286	K, B, M, L, I, H
18	13.31	$[M + HCOO]^-$	435.1505	435.1508	-0.9	$C_{17}H_{26}O_{10}$	Loganin	435.1505, 227.0910, 195.0637, 161.0388, 101.0235	L

TABLE 3: Continued.

No.	Retention time (min)	Ion species	Measured value (m/z)	Theoretical value (m/z)	Δ ppm	Molecular formula	Compound name	MS/MS	Source
19	14.00	$[M + H]^+$	634.2970	634.2970	1.4	$C_{31}H_{43}N_3O_{11}$	N1-dihydrocaffeoyl-N3-caffeoyl-spermidine-hexoside or isomer	634.2974, 472.2448, 382.1493, 310.2123, 220.0960, 163.0382	K
20	16.09	$[M + Cl]^-$	717.2164	717.2167	-0.5	$C_{32}H_{42}O_{16}$	Pinoresinoldiglucoside	717.2159, 681.2358, 519.1862, 357.1341, 199.0189	M
21	17.34	$[M - H]^-$	563.1399	563.1406	-1.3	$C_{26}H_{28}O_{14}$	Schaftoside	563.1400, 545.1725, 473.1082, 443.0978, 383.0765, 353.0650	H
22	17.56	$[M - H]^-$	563.1402	563.1406	-0.9	$C_{26}H_{28}O_{14}$	Isoschaftoside	563.1399, 545.1281, 473.1076, 443.0976, 383.0767, 353.0660	H
23	19.68	$[M - H]^-$	405.1192	405.1191	-0.2	$C_{20}H_{22}O_9$	2,3,5,4'-tetrahydroxystilbene-2-O- β -D-glucoside	243.0659, 225.0542, 173.0592, 137.0236, 93.0338	F
24	20.06	$[M - H]^-$	463.0876	463.0882	-1.3	$C_{21}H_{20}O_{12}$	Hyperoside	463.0868, 300.0269, 271.0233, 151.0023	E, B, M, K, A, M
25	22.93	$[M - H]^-$	515.1199	515.1195	0.3	$C_{25}H_{24}O_{12}$	Isochlorogenic acid B	515.1184, 353.0873, 191.0554, 173.0451, 135.0444	L, B, H
26	24.11	$[M - H]^-$	447.0928	447.0933	-1.0	$C_{21}H_{20}O_{11}$	Quercitrin	447.0919, 300.0268, 271.0238, 178.9975, 151.0025	E, B, C
27	24.66	$[M - H]^-$	515.1194	515.1195	-0.6	$C_{25}H_{24}O_{12}$	Isochlorogenic acid A	353.0872, 335.0758, 191.0553, 179.0342, 135.0445	L, B, M, H
28	25.00	$[M - H]^-$	269.0926	269.0932	-2.1	$C_{15}H_{14}N_2O_3$	Cuscutamine	269.0923, 225.1024, 183.0917, 156.0811	B
29	27.16	$[M - H]^-$	515.1199	515.1195	0.3	$C_{25}H_{24}O_{12}$	Isochlorogenic acid C	515.1185, 353.0875, 191.0556, 173.0450, 135.0440	L, B, M, H
30	29.45	$[M + Cl]^-$	835.4603	835.4616	1.9	$C_{42}H_{72}O_{14}$	Ginsenoside Rg1	835.4606, 799.4823, 179.0554,	A
31	37.14	$[M - H]^-$	1235.6083	1235.6066	1.13	$C_{59}H_{96}O_{27}$	Macranthoidin A	1235.6083, 1173.5550, 911.5005, 603.3802	L
32	38.16	$[M + NH_4]^+$	946.5404	946.537	3.2	$C_{47}H_{76}O_{18}$	Asperosaponin VI	946.5390, 786.9318, 455.3521, 437.3412, 295.1022,	L
33	38.79	$[M - H]^-$	329.2329	329.2333	-1.4	$C_{18}H_{34}O_5$	9,10,11-Trihydroxy-12-octadecanoic acid or isomer	329.2327, 293.2096, 211.1332, 171.1018, 139.1114	L, J
34	39.31	$[M + Cl]^-$	833.3948	833.3943	0.1	$C_{37}H_{66}O_{18}$	Cus 3	833.3939, 633.3480, 407.1564, 243.1952	B
35	39.89	$[M + Cl]^-$	833.3947	833.3943	0.1	$C_{37}H_{66}O_{18}$	Cus 3 isomer	833.3944, 633.3471, 407.1524, 243.1960	B
36	41.43	$[M - H]^-$	1163.5875	1163.5855	1.6	$C_{56}H_{92}O_{25}$	Malonylginsenoside Rb2 or Malonylginsenoside Rb3	1163.5863, 1119.5967, 1077.5869, 1059.5734	A
37	41.73	$[M + Cl]^-$	875.4042	875.4049	-0.3	$C_{39}H_{68}O_{19}$	Cus 1	875.4053, 633.3469, 407.1535, 243.1955	B

TABLE 3: Continued.

No.	Retention time (min)	Ion species	Measured value (m/z)	Theoretical value (m/z)	Δ ppm	Molecular formula	Compound name	MS/MS	Source
38	42.69	$[M + Cl]^-$	875.4042	875.4049	-0.3	$C_{39}H_{68}O_{19}$	Cus 1 isomer	875.4053, 633.3469, 407.1535, 243.1955	B
39	42.69	$[M + Cl]^-$	875.4042	875.4049	-0.3	$C_{39}H_{68}O_{19}$	Cus 1 isomer	875.4053, 633.3469, 407.1535, 243.1955	B
40	43.08	$[M + H]^+$	345.0979	345.0969	2.5	$C_{18}H_{16}O_7$	Eupatilin	345.0970, 330.0735, 315.0493, 269.0444, 169.0128	H
41	45.25	$[M + Cl]^-$	639.3664	639.3669	-0.7	$C_{35}H_{56}O_8$	Cauloside A	639.3660, 603.3887	L
42	45.74	$[M + H]^+$	233.1536	233.1536	0.2	$C_{15}H_{20}O_2$	Atractylenolide II	215.1427, 187.1480, 159.0801, 131.0852, 105.0696	I, J

A: Renshen; B: Tusizi; C: Sharen; D: Shudihuang; E: Sangjisheng; F: Show; G: Bajitian; H: Aiye; I: Baizhu; J: Dangshen; K: Gouqizi; L: Xuduan; M: Du Zhong.

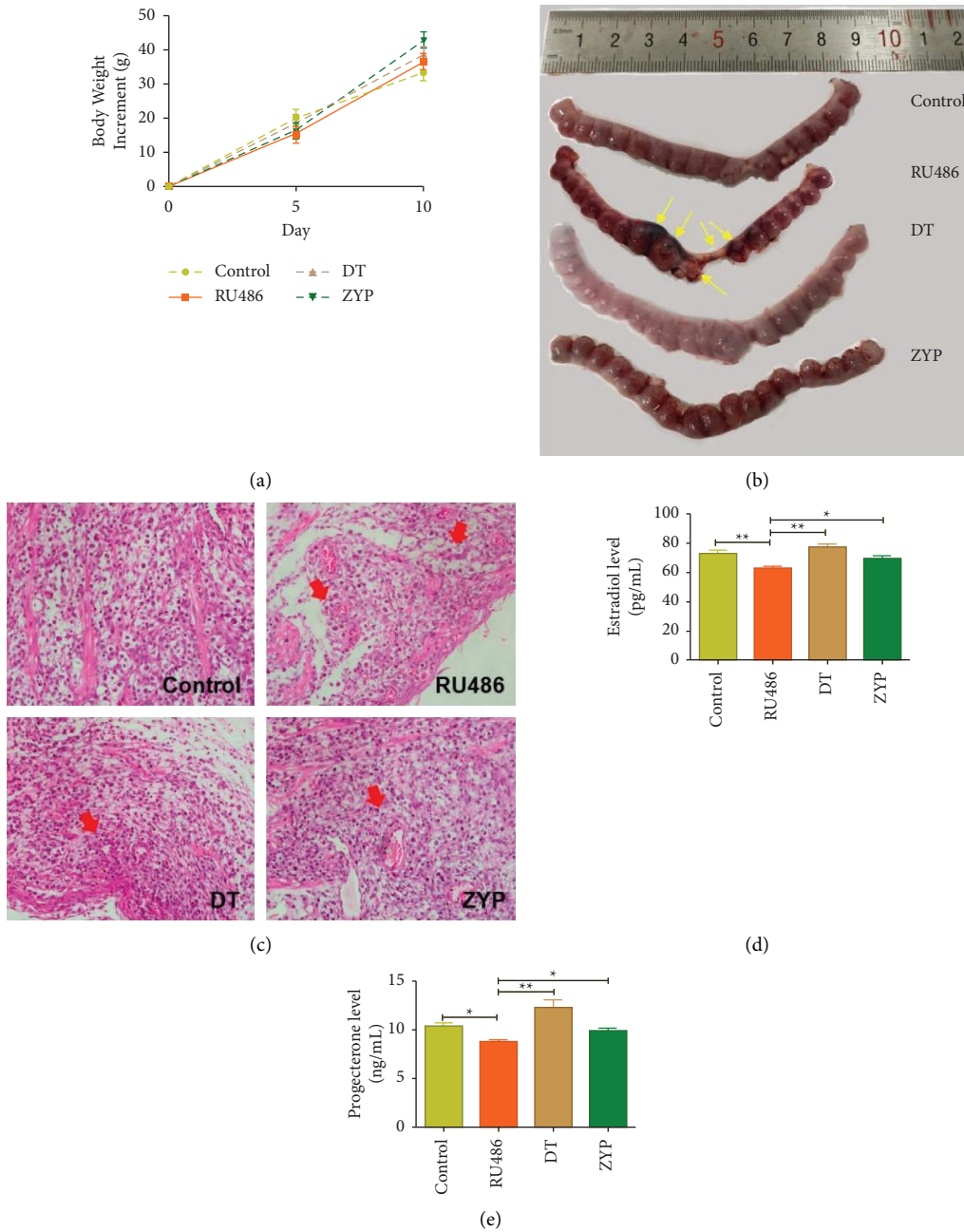


FIGURE 5: ZYP improves the general condition of rats in the RU486-induced TA model. (a) Body changes of rats in each group at 5th and 10th, respectively. (b) The images of the uterus in all groups of pregnant rats. (c) H&E staining was performed on the uterus to observe histopathologic changes. The red arrow represents histopathologic changes in the uterine section with the embryo. (d, e) Serum levels of E2 and P were detected by ELISA assay $n=6$, * $p < 0.05$, and ** $p < 0.01$.

RU486 compared to control. However, ZYP reduced the RU486-induced up-regulation of these genes. These results further demonstrated that ZYP could rescue RU486-induced TA by down-regulating the expression of genes involved in the PI3K/Akt pathway, the MAPK pathway, inflammation, and apoptosis.

3.10. Molecular Docking Result Analysis. Molecular docking analysis was conducted to assess the binding affinity of

compounds with their target receptor; the docking score produced represented an index of molecular docking. A lower score indicated that the binding affinity was stronger. We used AutoDock Vina to perform molecular docking for all key compounds and hub target proteins; the results are represented by heat maps (Figure 7(a)). Data showed that the docking scores of key compounds with major hub target proteins ranged from -2.2 to -10.6. In particular, GinsenosideRg5-qt was docked with TNF- α , Cauloside A-qt was docked with CAS3, Spinasterol was docked with

MAPK1, rhein was docked with *MAPK3*, Ginsenoside-Rh4-qt and Aposiopolamine were docked with *MAPK8*, chrysohanol was docked with *MAPK14*, and emodin was docked with *PIK3CA*, with docking scores of -8.8 , -8.4 , -8.8 , -9.7 , -10.4 , -10.4 , and -9.5 kcal/mol, respectively, (Figure 7(b)).

4. Discussion

It is well acknowledged that traditional Chinese medicine plays a significant role in medicine and health worldwide. However, the pharmacological mechanisms associated with TCM are often ambiguous due to the complexity of the components involved [30]. The use of network pharmacology, a tool that is based on bioinformatics and the concept of “Disease-Gene-Target-Medicine,” now provides us with an efficient platform with which to elucidate the molecular mechanism that underlies the action of TCM [35, 36]. We conducted an integrative analysis based on network pharmacology to investigate the mechanisms associated with the action of ZYP on TA and then used an animal model to verify our results. We indicated that ZYP might affect TA by regulating the MAPK and PI3K/Akt pathways and by inhibiting the expression levels of genes associated with proinflammatory cytokines and apoptosis.

Here, we present data derived from the network pharmacology analysis of ZYP on TA for the first time. We analyzed the chemical composition of ZYP by UPLC-Q-TOF/MS and identified 42 compounds based on the information of the multilevel mass spectra of the sample, combined with the natural product high-resolution mass spectrometry database and related literature. We also used an RU486-induced rat model of TA to verify the effect of ZYP on TA, as predicted by network pharmacology. We identified 1363 compounds in the 15 herbs that make up ZYP from the TCMSP database and the Shanghai Institute of Organic Chemistry of the Chinese Academy of Sciences Chemistry Database. In total 161 compounds were selected by ADME. We identified 1025 target proteins using PubChem and Swiss Target Prediction. Using the GeneCards database, we identified 1732 TA-associated target genes. Based on these target compounds and genes, and by combining these data with PPI data from STRING, we identified the top 41 putative target genes for GO biological process and KEGG pathway enrichment analyses. In total, 22 KEGG pathways were identified, after which compound-target-pathway networks were then constructed and integrated. Molecular docking also indicated that the active compounds may have high binding affinities to the proteins encoded by the TA-related genes. After identifying the potential pathway by way of network pharmacology, we further verified the authenticity of the network analysis results by carrying out experiments *in vivo*. We also explored the mechanisms that may underline the action of ZYP on TA.

The MAPK signaling pathway is known to be related to a series of physiological and pathological processes, such as development, cell growth, and endocrine diseases [37, 38]. The MAPK pathway also plays a key role in the maintenance of normal pregnancies in the reproductive system. There are four independent signaling cascades, including the *JNK*,

ERK, *P38MAPK*, and *ERK5* cascades. Evidence has shown that smoking-induced oxidative stress can activate the *P38MAPK* signal pathway and thereby weaken the normal development of trophoblast cells [36]. Total flavones extracted from *Cuscuta Chinensis* were also shown to significantly down-regulated the expression levels of *ERK* and *P38* in decidua tissue from spontaneous abortions and could reverse the decidual damage caused by RU486 and effectively reduce the rate of miscarriage [34]. Consistent with a previous study, our studies showed that the expression levels of genes associated with the MAPK pathway (*Erk1*, *Erk2*, *Mapk14*, and *Jnk*) were remarkably down-regulated in the RU486-induced rat model of TA. We speculate that ZYP could significantly interfere with the overactivated MAPK pathway to mediate its antiabortion effect.

The PI3K/Akt pathway is a classic mitochondrial apoptosis pathway and regulates various biological processes, including transcription, cell growth, migration, apoptosis, motility, and metabolism [39, 40]. The relationship between miscarriage and the PI3K/Akt pathway has been studied for decades. Previous studies have shown that the PI3K/Akt signaling pathway by activating participates in the proliferation of trophoblast cells, protects trophoblasts, inhibits apoptosis, and promotes cell viability [41–44]. In addition, this pathway can help to regulate female gamete development and improve embryo implantation [45]. Thus, the PI3K/Akt signaling pathway plays a critical role in establishing and maintaining a successful pregnancy [46]. However, our biological verification data, produced by qRT-PCR, identified an interesting phenomenon. In contrast to previous results, our study found that RU486 resulted in significantly increased mRNA levels of *Pi3kca* and *Akt*, while ZYP treatment reversed RU486-induced overactivation of the PI3K/Akt pathway. The reason for this result may be that the PI3K/Akt signaling pathway may be activated as a stress compensatory mechanism in RU486-induced TA, while overactivation leads to the dysfunction of compensatory function in the body and a decline in the function of cells to maintain homeostasis. Therefore, inhibiting the excessive activation of the PI3K/Akt signaling pathway could effectively improve the symptoms of TA.

Previous studies have shown that many proinflammatory cytokines (including *IL6* and *TNF- α*) play active roles in inflammation and immunity and that their overproduction may cause obstetric disorders, such as abortion or preterm birth [47, 48]. Consistent with a previous study, our studies showed that the expression levels of inflammation-associated genes (*IL6* and *TNF- α*) were significantly up-regulated in the RU486-induced rat model of TA. However, ZYP could down-regulated the expression levels of *IL6* and *TNF- α* , and inhibited inflammation. We also detected the expression levels of apoptosis-related cytokines, including *Cas3* and *Cas8*, by qRT-PCR. Consistent with KEGG enrichment results, the level of apoptosis was inhibited in the ZYP group accompanied by reduced expression levels of *Cas3* and *Cas8* expression. Data suggested that the active compounds might have high binding affinities for the proteins encoded by TA-related genes, thus confirming the mechanisms underlying the action of ZYP on TA. RU486 significantly activated the PI3K/Akt pathway and MAPK pathway and caused inflammation and apoptosis, while

ZYP treatment reversed RU486-induced apoptosis and abortion.

5. Conclusion

In this study, we used network pharmacology to reveal the mechanisms underlying the action of ZYP on TA for the first time. We demonstrated that ZYP may exert action on TA by modulating the PI3K/Akt, MAPK, and TNF signaling pathways, and apoptosis. Subsequently, *in vivo* experiments verified the convincing evidence that the network pharmacology method provided and revealed the potential mechanisms underlying the action of ZYP on TA. We found that ZYP may inhibit the PI3K/Akt and MAPK signaling pathways, while also inhibiting inflammation, apoptosis, and the development of TA. In this study, we used a network pharmacology method to initially reveal the potential pharmacological mechanism of multitarget and multipathway interventions of ZYP on TA, which provides a scientific basis for a comprehensive understanding of the pharmacological effects of ZYP.

Abbreviation

TA:	Threatened abortion
ZYP:	Zishen Yutai Pill
PPI:	Protein-protein interaction
GO:	Gene ontology
KEGG:	Kyoto Encyclopedia of Genes and Genomes
TCM:	Traditional Chinese Medicine
OB:	Oral bioavailability
DL:	Drug-likeness
E2:	Estradiol
P:	Progesterone
SD:	Sprague-Dawley
DT:	Dydrogesterone.

Data Availability

The data used to support the findings of this study are included within the supplementary information files.

Conflicts of Interest

The authors declare that there are no conflicts of interest.

Authors' Contributions

Jiazhen Wang (J.W.) analyzed the data and wrote the paper. Xin Liu (X.L.) performed the research and wrote the paper. Yougang Zhang (Y.Z.), Shenghua Lin (S.L.), Ting Lei (T.L.), Chen Sun (C.S.), and Kechun Liu (K.L.) were supportive during the experiment. Qiuxia He (Q.H.) designed and performed the study. All authors have read and agreed to the published version of the manuscript. Jiazhen Wang and Xin Liu have contributed equally.

Acknowledgments

This work was financially supported by the Funding of the National Key R&D Program of China (Grant no.

2018YFC1707300), Science, Education, and Industry Integration Innovation Pilot Project of Qilu University of Technology (Shandong Academy of Sciences) (Grant no. 2020KJC-ZD10), and Major Scientific and Technological Innovation Program of Shandong Province (Grant no. 2019JZZY021020).

Supplementary Materials

Supplementary Tables: The candidate targets for ZYP were imported into the DAVID database for GO functional enrichment analysis and KEGG signaling pathway enrichment analysis. The analysis identified a range of GO terms, including biological process (BP), molecular function (MF), and cellular components (CC). The authors identified 169 BPs, 17 CCs, and 32 MFs of significance ($p < 0.05$, and $FDR < 0.05$, Supplementary Tables S1–S3). To further identify the potential mechanisms underlying the effect of ZYP on TA, we conducted the KEGG pathway enrichment analysis and identified 104 pathways in the DAVID database ($p < 0.05$, and $FDR < 0.05$, Supplementary Table S4). Graphical abstract: first, we identified the chemical constituents of ZYP from multiple databases and then predicted the potential targets of TA by applying the GeneCards database. A protein-protein interaction (PPI) network was then constructed to allow the screening of hub targets. Gene Ontology (GO) and Kyoto Encyclopedia of Genes and Genomes (KEGG) enrichment analyses were also performed and the Database for Annotation Visualization and Integrated Discovery server was used to identify critical biological processes and signaling pathways. Cytoscape software was used to construct a Compound-Target-Pathway. Finally, a rat model of TA induced by RU486 was established, and the reliability of the network pharmacology prediction results was verified. Finally, the mechanisms responsible for the action of ZYP on TA were revealed by qRT-PCR and molecular docking. (*Supplementary Materials*)

References

- [1] S. Amrane and R. McConnell, "Endocrine causes of recurrent pregnancy loss," *Seminars in Perinatology*, vol. 43, no. 2, pp. 80–83, 2019.
- [2] C. Ban, M. Jo, YH. Park et al., "Enhancing the oral bioavailability of curcumin using solid lipid nanoparticles," *Food Chemistry*, vol. 302, Article ID 125328, 2020.
- [3] G. Barrientos, D. Fuchs, K. Schröcksnadel et al., "Low levels of serum asymmetric antibodies as a marker of threatened pregnancy," *Journal of Reproductive Immunology*, vol. 79, no. 2, pp. 201–210, 2009.
- [4] H. Cakmak and H. S. Taylor, "Implantation failure: molecular mechanisms and clinical treatment," *Human Reproduction Update*, vol. 17, no. 2, pp. 242–253, 2011.
- [5] J. Calleja-Agius, S. Muttukrishna, A. R. Pizzey, and E. Jauniaux, "Pro- and antiinflammatory cytokines in threatened miscarriages," *American Journal of Obstetrics and Gynecology*, vol. 205, no. 1, pp. 8–83, 2011.
- [6] T. Cao, D. Yang, X. Zhang et al., "FAM3D inhibits glucagon secretion via MKP1-dependent suppression of ERK1/2 signaling," *Cell Biology and Toxicology*, vol. 33, no. 5, pp. 457–466, 2017.

- [7] H. Carp, "A systematic review of dydrogesterone for the treatment of recurrent miscarriage," *Gynecological Endocrinology*, vol. 31, no. 6, pp. 422–430, 2015.
- [8] C. Everett, "Incidence and outcome of bleeding before the 20th week of pregnancy: prospective study from general practice," *BMJ*, vol. 315, no. 7099, pp. 32–34, 1997.
- [9] X. Feng, S. Jiang, W. Leung et al., "BuShen HuoXue decoction promotes decidual stromal cell proliferation via the PI3K/AKT pathway in unexplained recurrent spontaneous abortion," *Evidence-based Complementary and Alternative Medicine*, vol. 2020, Article ID 6868470, 11 pages, 2020.
- [10] Q. Gao, L. Han, X. Li, and X. Cai, "Traditional Chinese medicine, the zishen Yutai pill, ameliorates precocious endometrial maturation induced by controlled ovarian hyperstimulation and improves uterine receptivity via upregulation of HOXA10," *Evidence-based Complementary and Alternative Medicine*, vol. 2015, Article ID 317586, 10 pages, 2015.
- [11] S. Giakoumelou, N. Wheelhouse, K. Cuschieri, G. Entrican, S. E. Howie, and A. W. Horne, "The role of infection in miscarriage," *Human Reproduction Update*, vol. 22, no. 1, pp. 116–133, 2016.
- [12] F. Gómez-Chávez, V. Castro-Leyva, A. Espejel-Núñez et al., "Galectin-1 reduced the effect of LPS on the IL-6 production in decidual cells by inhibiting LPS on the stimulation of $\text{I}\kappa\text{B}\zeta$," *Journal of Reproductive Immunology*, vol. 112, pp. 46–52, 2015.
- [13] A. L. Hopkins, "Network pharmacology," *Nature Biotechnology*, vol. 25, no. 10, pp. 1110–1111, 2007.
- [14] A. L. Hopkins, "Network pharmacology: the next paradigm in drug discovery," *Nature Chemical Biology*, vol. 4, no. 11, pp. 682–690, 2008.
- [15] da W. Huang, B. T. Sherman, and R. A. Lempicki, "Systematic and integrative analysis of large gene lists using DAVID bioinformatics resources," *Nature Protocols*, vol. 4, no. 1, pp. 44–57, 2009.
- [16] E. Ipsa, V. F. Cruzat, J. N. Kagize, J. L. Yovich, and K. N. Keane, "Growth hormone and insulin-like growth factor action in reproductive tissues," *Frontiers in Endocrinology*, vol. 10, p. 777, 2019.
- [17] J. Ji, L. Chen, Y. Zhuang, Y. Han, W. Tang, and F. Xia, "Fibronectin 1 inhibits the apoptosis of human trophoblasts by activating the PI3K/Akt signaling pathway," *International Journal of Molecular Medicine*, vol. 46, pp. 1908–1922, 2020.
- [18] L. Li, N. Ning, J. A. Wei et al., "Metabonomics study on the infertility treated with zishen Yutai pills combined with *in vitro* fertilization-embryo transfer," *Frontiers in Pharmacology*, vol. 12, Article ID 686133, 2021.
- [19] Y. E. Li, L. Zeng, Y. H. Li, and Q. L. Wu, "Effect of zishen Yutai pill combined with diane-35 on polycystic ovary syndrome," *Prac Clin Med*, vol. 20, pp. 44–46, 2019.
- [20] Z. Li, G. Zhou, L. Jiang, H. Xiang, and Y. Cao, "Effect of STOX1 on recurrent spontaneous abortion by regulating trophoblast cell proliferation and migration via the PI3K/AKT signaling pathway," *Journal of Cellular Biochemistry*, vol. 120, no. 5, pp. 8291–8299, 2018.
- [21] CE. Lim, KK. Ho, NC. Cheng, and F. W. Wong, "Combined oestrogen and progesterone for preventing miscarriage," *Cochrane Database of Systematic Reviews*, vol. 2013, pp. 9278–45, 2013.
- [22] L. Lu, S. Zhan, X. Liu, X. Zhao, X. Lin, and H. Xu, "Antitumor effects and the compatibility mechanisms of herb pair *Scleromitrium diffusum* (willd.) R. J. Wang-*Scullellaria barbata* D. Don," *Frontiers in Pharmacology*, vol. 11, p. 292, 2020.
- [23] C. Ma, L. Wang, and X. Q. Xie, "GPU accelerated chemical similarity calculation for compound library comparison," *Journal of Chemical Information and Modeling*, vol. 51, no. 7, pp. 1521–1527, 2011.
- [24] G. Makrydimas, NJ. Sebire, D. Lolis, N. Vlassis, and K. H. Nicolaides, "Fetal loss following ultrasound diagnosis of a live fetus at 6–10 weeks of gestation," *Ultrasound in Obstetrics and Gynecology*, vol. 22, no. 4, pp. 368–372, 2003.
- [25] A. Mauri, V. Consonni, M. Pavan, and R. Todeschini, "Dragon software: an easy approach to molecular descriptor calculations," *Match-Commun Math Co*, vol. 56, pp. 237–248, 2006.
- [26] R. Menon and J. Papaconstantinou, "p38 Mitogen activated protein kinase (MAPK): a new therapeutic target for reducing the risk of adverse pregnancy outcomes," *Expert Opinion on Therapeutic Targets*, vol. 20, no. 12, pp. 1397–1412, 2016.
- [27] Practice Committee of the American Society for Reproductive Medicine, "Evaluation and treatment of recurrent pregnancy loss: a committee opinion," *Fertility and Sterility*, vol. 98, no. 5, pp. 1103–1111, 2012.
- [28] JR. Prins, N. Gomez-Lopez, and S. A. Robertson, "Interleukin-6 in pregnancy and gestational disorders," *Journal of Reproductive Immunology*, vol. 95, no. 1–2, pp. 1–14, 2012.
- [29] A. E. Ridout, L. A. Ibeto, GN. Ross et al., "Cervical length and quantitative fetal fibronectin in the prediction of spontaneous preterm birth in asymptomatic women with congenital uterine anomaly," *American Journal of Obstetrics and Gynecology*, vol. 221, no. 4, pp. 1–341, 2019.
- [30] P. Shannon, A. Markiel, O. Ozier et al., "Cytoscape: a software environment for integrated models of biomolecular interaction networks," *Genome Research*, vol. 13, no. 11, pp. 2498–2504, 2003.
- [31] W. Tao, X. Xu, X. Wang et al., "Network pharmacology-based prediction of the active ingredients and potential targets of Chinese herbal Radix Curcumae formula for application to cardiovascular disease," *Journal of Ethnopharmacology*, vol. 145, no. 1, pp. 1–10, 2013.
- [32] WP. Walters and M. A. Murcko, "Prediction of 'drug-likeness,'" *Advanced Drug Delivery Reviews*, vol. 54, no. 3, pp. 255–271, 2002.
- [33] Z. Wang, X. Liu, J. Xu et al., "Paternal age, body mass index, and semen volume are associated with chromosomal aberrations-related miscarriages in couples that underwent treatment by assisted reproductive technology," *Aging*, vol. 12, no. 9, pp. 8459–8472, 2020.
- [34] D. S. Wishart, Y. D. Feunang, A. C. Guo et al., "DrugBank 5.0: a major update to the DrugBank database for 2018," *Nucleic Acids Research*, vol. 46, no. 1, pp. 1074–1082, 2018.
- [35] J. Liu, J. Liu, X. Tong et al., "Network pharmacology prediction and molecular docking-based strategy to discover the potential pharmacological mechanism of huai hua san against ulcerative colitis," *Drug Design, Development and Therapy*, vol. 15, pp. 3255–3276, 2021.
- [36] Y. Dong, Q. Zhao, and Y. Wang, "Network pharmacology-based investigation of potential targets of astragalus membranaceous-angelica sinensis compound acting on diabetic nephropathy," *Scientific Reports*, vol. 11, no. 1, Article ID 19496, 2021.
- [37] HW. Wu, YH. Feng, DY. Wang et al., "Effect of total flavones from *Cuscuta Chinensis* on anti-abortion via the MAPK signaling pathway," *Evidence-based Complementary and Alternative Medicine*, vol. 2018, Article ID 6356190, 12 pages, 2018.
- [38] W. Wu, S. Yang, P. Liu, L. Yin, Q. Gong, and W. Zhu, "Systems pharmacology-based strategy to investigate pharmacological mechanisms of Radix puerariae for treatment of hypertension," *Frontiers in Pharmacology*, vol. 11, p. 345, 2020.

- [39] H. O. Xu and Y. L. Luo, "Application of Zishen Yutai pills on Polycystic ovary syndrome ovulation induction," *Chinese Journal of information on TCM*, vol. 15, p. 68, 2008.
- [40] Y. Yamanishi, M. Kotera, M. Kanehisa, and S. Goto, "Drug-target interaction prediction from chemical, genomic and pharmacological data in an integrated framework," *Bioinformatics*, vol. 26, no. 12, pp. 246–254, 2010.
- [41] B. Y. Yang, J. W. Song, H. Z. Sun et al., "PSMB8 regulates glioma cell migration proliferation, and apoptosis through modulating ERK1/2 and PI3K/AKT signaling pathways," *Biomedicine and Pharmacotherapy*, vol. 100, pp. 205–212, 2018.
- [42] S. Yang, J. Zhang, Y. Yan et al., "Network pharmacology-based strategy to investigate the pharmacologic mechanisms of *Atractylodes macrocephala koidz.* For the treatment of chronic gastritis," *Frontiers in Pharmacology*, vol. 10, p. 1629, 2020.
- [43] C. Zhang, R. Liang, X. Gan, X. Yang, L. Chen, and J. Jian, "MicroRNA-384-5p/Beclin-1 as potential indicators for epigallocatechin gallate against cardiomyocytes ischemia reperfusion injury by inhibiting autophagy via PI3K/Akt pathway," *Drug Design, Development and Therapy*, vol. 13, pp. 3607–3623, 2019.
- [44] W. H. Zhang, X. D. Lan, and Y. H. Zhou, "Clinical efficacy of Zishen Yutai Wan plus progesterone injection on threatened abortion," *Clin J Chin Med*, vol. 11, pp. 94–96, 2019.
- [45] Y. Zhang, W. Yan, P. F. Ge, Y. Li, and Q. Ye, "Study on prevention effect of Zishen Yutai pill combined with progesterone for threatened abortion in rats," *Asian Pacific Journal of Tropical Medicine*, vol. 9, no. 6, pp. 577–581, 2016.
- [46] Z. Zhou and J. Y. Lei, "Clinical Observation on the treatment of luteal phase defect menstrual disorder by Zishen Yutai Pill," *Liaoning J Tradit Chin Med*, vol. 34, pp. 1694–1696, 2008.
- [47] R. Zhu, Y. H. Huang, Y. Tao et al., "Hyaluronan up-regulates growth and invasion of trophoblasts in an autocrine manner via PI3K/AKT and MAPK/ERK1/2 pathways in early human pregnancy," *Placenta*, vol. 34, no. 9, pp. 784–791, 2013.
- [48] W. J. Zhu, X. M. Li, X. M. Chen, and L. Zhang, "Effect of Zishen Yutai pill on embryo implantation rate in patients undergoing fertilization embryo transfer in vitro," *Chinese Journal of Integrated Traditional and Western Medicine*, vol. 20, pp. 729–737, 2002.